

## Exploring the characteristics of SnO<sub>2</sub> nanoparticles doped organic blend for low cost nanoelectronics applications

A.J.K. Algidsawi<sup>1</sup>, A. Hashim<sup>2</sup>, A. Hadi<sup>3</sup>, M.A. Habeeb<sup>2</sup>

<sup>1</sup>Department of Soil and Water, College of Agriculture, AL-Qasim Green University, Babylon, Iraq

<sup>2</sup>Department of Physics, College of Education of Pure Sciences, University of Babylon, Babylon, Iraq

<sup>3</sup>University of Babylon, College of Materials Engineering, Department of Ceramic and Building Materials, Iraq

E-mail: ahmed\_taay@yahoo.com

**Abstract.** The PVA/PVP/SnO<sub>2</sub> nanostructure films were fabricated using the casting technique. The structure, dielectric and optical characteristics of PVA/PVP/SnO<sub>2</sub> nanostructures were studied for pressure sensors. Results of studying the dielectric characteristics showed that the dielectric constant, dielectric losses and electrical conductivity of blend are enhanced with the rise of SnO<sub>2</sub> nanoparticles (NPs) content. The dielectric constant and dielectric losses are reduced, while the conductivity is risen with the increase in frequency. The dielectric constant increases from 2.53 to 7.41, and dielectric losses rise from 0.5 to 2, while the conductivity increases from  $2.82 \cdot 10^{-11}$  S/cm up to  $1.11 \cdot 10^{-10}$  S/cm. The results of measuring the optical characteristics have indicated that the absorbance rises with increasing the SnO<sub>2</sub> NPs content. The energy gap of blend has been reduced from 4.9 down to 4.65 eV with the rise in SnO<sub>2</sub> NPs content. The optical constants have been improved with the rise in SnO<sub>2</sub> NPs content. Results of studying the pressure sensors have shown that their capacitance grows with the pressure increase.

**Keywords:** SnO<sub>2</sub>, pressure sensors, capacitance, energy gap, nanocomposites.

<https://doi.org/10.15407/spqeo24.04.472>

PACS 07.07.Df, 78.67.Bf, 81.07.-b

Manuscript received 01.05.21; revised version received 01.08.21; accepted for publication 10.11.21; published online 23.11.21.

### 1. Introduction

In the recent years, polymer materials have been a subject of significant interest because of their chemical and physical characteristics. Polymers are generally employed in electrical insulation industry as well as in microelectronics. Various films of polymers, *e.g.*, pure polymers and those doped with various additives, are employed in different technological, biological and medical applications [1]. In the type of novel materials, polymeric nanocomposites include huge grabbing attention related to their improved optical, electrical and magnetic characteristics. These materials demonstrate rising modulus and flame resistance and also are capable to prevent agglomeration and oxidation. This improvement in characteristics is related with interaction between polymer and nanoparticles. Addition of nanoparticles to polymer enhances nanoparticles' life time, modifies the nanoparticles surface with passivation of defect levels, provides low cost, easy device fabrication as well as tunable electronic and optical characteristics. Polyvinyl alcohol (PVA) among the other polymers is one of the main representatives and useful polymer. PVA is colorless and water soluble. It exhibits characteristics such as biocompatibility as well as chemical and thermal

stability. Therefore, PVA is typically employed in the applications like paper coating, surfactants, drug delivery, films, and glues. The good transparency in the entire range of visible spectrum makes PVA a good candidate in nonlinear optical fields, such as optical bistability and creation of optical harmonics [2]. PVP is excellent forming films and behaves as an adhesive on several solid substrates. It promotes appearance of films with excellent optical quality and mechanical strength, which is essential for various fields. The PVP amorphous structure also shows a low light scattering, which makes it to be a perfect polymer for various applications [3]. In previous over two decades, nanosize semiconducting oxides attracted a large interest related to their application in optoelectronic devices, sensing, or catalysis. These materials merging high transparency with excellent electrical conductivity include several various fields in emerging and contemporary technologies like to optoelectronic devices for nonemissive and emissive information displays [4]. SnO<sub>2</sub> is usually employed in various applications due to its high transparency and electrical conductivity, low cost, high infrared reflectivity, superior chemical stability. The stoichiometric SnO<sub>2</sub> is an excellent insulator, but nonstoichiometry

relates it to *n*-type semiconductors with intrinsic defects [5]. SnO<sub>2</sub> is of *n*-type, large band gap (about 3.5 eV) semiconductor and in the thin films form, it is a transparent conducting matter that shows the high optical transmission (80...90%). The transparent conducting SnO<sub>2</sub> thin films are employed as electrodes in various optoelectronic devices, as heat mirror coatings, buildings smart windows, airplane and automobile windshields, incandescent light bulbs, flat plate and concentrating solar collectors [6]. There are studies on pressure sensors that were fabricated from nanocomposites [7–9]. This paper aims to fabricate PVA/PVP/SnO<sub>2</sub> nanostructures to be used as a new pressure sensor having the low cost, flexibility, light weight and high sensitivity.

## 2. Materials and methods

The materials used in this work include: tin oxide nanopowder (SnO<sub>2</sub>, high purity 99.7%, 35...55 nm, US Research Nanomaterials, Inc., USA), polyvinyl alcohol (PVA) and polyvinyl pyrrolidone (PVP). The PVA-PVP-SnO<sub>2</sub> NPs films were fabricated by using the casting method. The polymers solution prepared by dissolving of 1 g of PVA and PVP in distilled water (40 ml) with the ratio 65 wt.% PVA:35 wt.% PVP. The SnO<sub>2</sub> nanoparticles (NPs) were added to solution with contents 2, 4 and 6 wt.%. The optical characteristics were tested within the wavelength range from 220 up to 820 nm by using spectrophotometer (UV/1800/ Shimadzu). The dielectric characteristics of PVA/PVP/SnO<sub>2</sub> nanostructures were measured in frequency from 100 Hz to 5·10<sup>6</sup> Hz by LCR meter type (HIOKI 3532-50 LCR HI TESTER). The pressure sensor application for nanostructures were tested by measuring the capacitance (*C<sub>p</sub>*) between two electrodes on the bottom and top sides of the film with various pressures ranging from 80 up to 200 bar.

The absorption coefficient *α* can be defined using the equation [10, 11]:

$$\alpha = 2.303 (A/t), \quad (1)$$

where *A* is the absorbance and *t* – thickness of the sample.

The energy band gap calculated using Eq. [12]:

$$\alpha h\nu = B(h\nu - E_g)^r, \quad (2)$$

where *B* is a constant, *hν* – photon energy, *E<sub>g</sub>* – energy band gap, *r* = 3 for forbidden indirect transition, and *r* = 2 for allowed indirect transition.

The refractive index *n* is defined by the equation [12]:

$$n = \frac{1 + \sqrt{R}}{1 - \sqrt{R}}, \quad (3)$$

where *R* is the reflectance.

The extinction coefficient *k* is given by [13]:

$$k = \frac{\alpha\lambda}{4\pi}, \quad (4)$$

where *λ* is the wavelength of incident photons.

The real *ε<sub>1</sub>* and imaginary *ε<sub>2</sub>* dielectric constant parts can be calculated by [14, 15]:

$$\epsilon_1 = n^2 - k^2, \quad (5)$$

$$\epsilon_2 = 2nk. \quad (6)$$

The optical conductivity *σ<sub>op</sub>* can be determined by the equation [16–18]

$$\sigma_{op} = \frac{\alpha n C}{4\pi}. \quad (7)$$

The dielectric constant *ε'* was calculated using the equation [19]:

$$\epsilon' = \frac{C_p}{C_0}, \quad (8)$$

where *C<sub>p</sub>* is the capacitance and *C<sub>0</sub>* – vacuum capacitance.

The dielectric loss *ε''* was defined by using the equation [20]:

$$\epsilon'' = \epsilon' D, \quad (9)$$

where *D* is the dispersion factor.

The AC electrical conductivity can be determined using the expression [21]:

$$\sigma_{AC} = w \cdot \epsilon'' \cdot \epsilon_0, \quad (10)$$

where *w* is the angular frequency.

## 3. Results and discussion

The absorbance spectra of pure blend PVA/PVP and SnO<sub>2</sub> NPs dispersed PVA/PVP are given in Fig. 1. It is well recognized that pure blend absorbs the radiation strongly within the wavelength range 220...400 nm. The shift in both absorption bands and the band edges towards the higher wavelengths with various absorption intensities for various content of doped PVA/PVP films. These absorption band shifts offer the formation idea of inter-/intramolecular hydrogen bonding presented between SnO<sub>2</sub> ions with the adjacent OH groups of the PVA/PVP chain. The rise in absorption is mostly related to the rise in SnO<sub>2</sub> content causing more and more inter-/intra-hydrogen bonding. This may be enlightened additionally

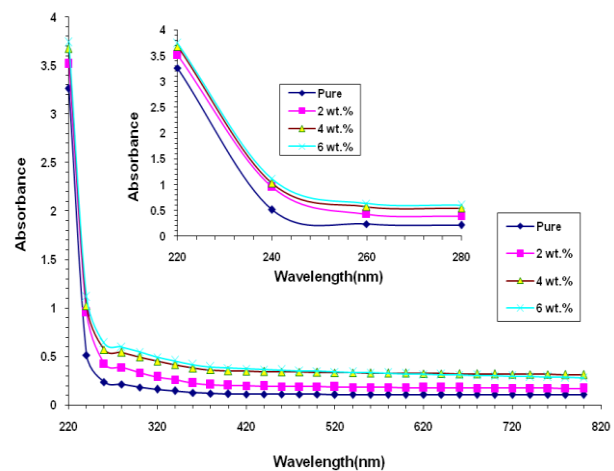
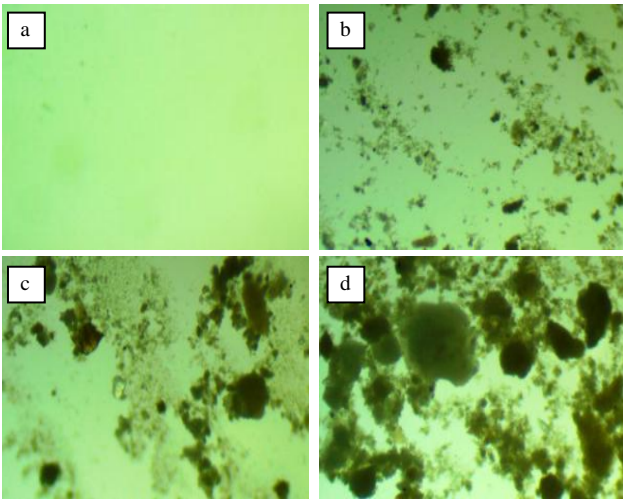
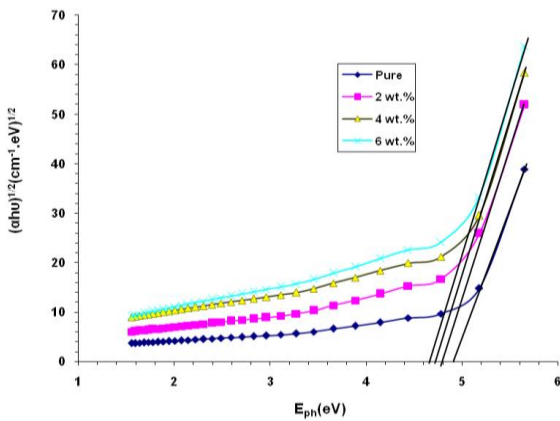


Fig. 1. Absorbance spectra of PVA/PVP/SnO<sub>2</sub> nanostructures.



**Fig. 2.** Optical microscope images of PVA/PVP/SnO<sub>2</sub> nanostructures ( $\times 10$ ): (a) pure blend, (b) 2 wt.% SnO<sub>2</sub>, (c) 4 wt.% SnO<sub>2</sub>, and (d) 6 wt.% SnO<sub>2</sub>.



**Fig. 3.** Energy band gap values for the allowed transition.

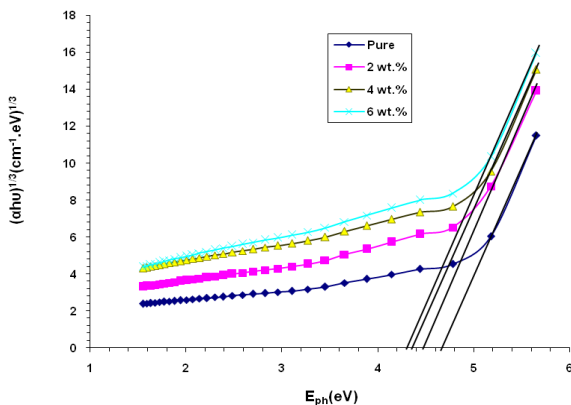


**Fig. 4.** Energy band gap values for the forbidden transition.

by using the Beer law that indicates the radiation absorption is directly proportional to the absorbing molecules number in the films. The shift witnessed in the absorption edge of the doped PVA/PVP is fundamentally related to variation in crystalline parameters, which, in turn, changes the energy gap [22]. Also, the increase in absorption

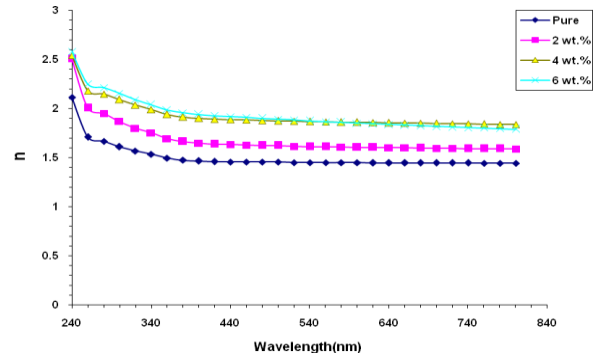


**Fig. 5.** Variation of refractive index of PVA/PVP/SnO<sub>2</sub> nanostructures with changing the wavelength.

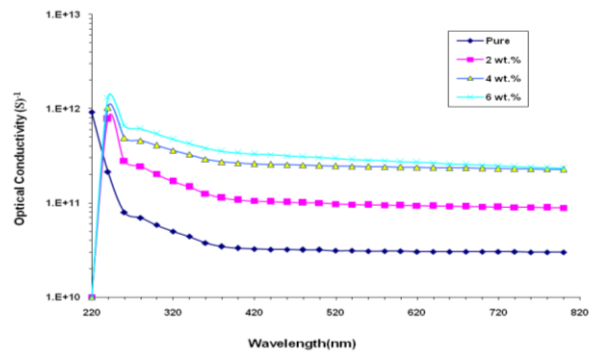


**Fig. 6.** Variation of optical conductivity for PVA/PVP/SnO<sub>2</sub> nanostructures with changing the wavelength.

due to increase of charge carriers number inside the nanocomposite [23], as shown in Fig. 2 that demonstrates the distribution of SnO<sub>2</sub> NPs inside the PVA/PVP matrix.

Figs 3 and 4 represent the energy gap of allowed and forbidden indirect transitions. As shown in Figs 3 and 4, the energy gap reduces with the increase in SnO<sub>2</sub> content. This decrease in the values of optical energy is related to formation of defects and, therefore, influences the optical characteristics of materials. In the considered range of wavelengths, the absorption bands are associated with  $\pi-\pi^*$  electron transition. The  $\pi$ -electron excitation requires smaller energy and, consequently, this transition occurs at higher wavelengths. This decrease in the band gap value can be related to the presence of unstructured defects, which rises the localized levels density in the band gap [24, 25]. Fig. 5 represents refractive index variation of PVA/PVP/SnO<sub>2</sub> nanostructures with changing the wavelength. The refractive index rises with increasing the SnO<sub>2</sub> NPs content; it is reduced with the rise of wavelength. This behavior is related with the rise of the film density. When the incident light that interacts with the film has high refractivity in UV region, the refractive index values will be increased [26].

Variation of the optical conductivity inherent to PVA/PVP/SnO<sub>2</sub> nanostructures with changing the wavelength is shown in Fig. 6. The optical conductivity of blend rises with the rise in SnO<sub>2</sub> NPs content. The optical conductivity of PVA/PVP/SnO<sub>2</sub> nanostructures rises with the rise in energy corresponding to the band gap, which is related with electrons excited by photon energy and provides the high absorption coefficient [27].

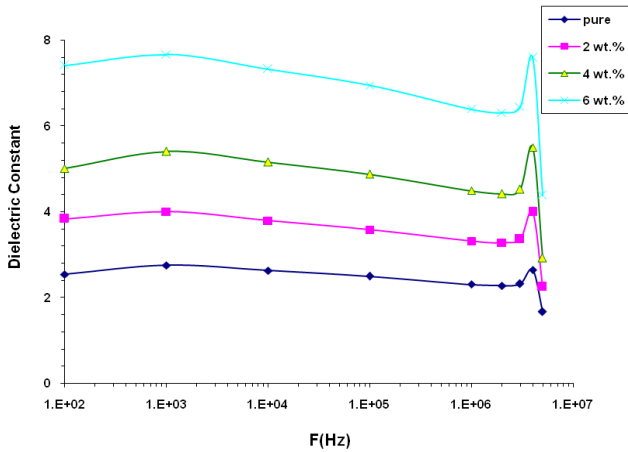


**Fig. 7.** Variation of dielectric constant of PVA/PVP/SnO<sub>2</sub> nanostructures with frequency.

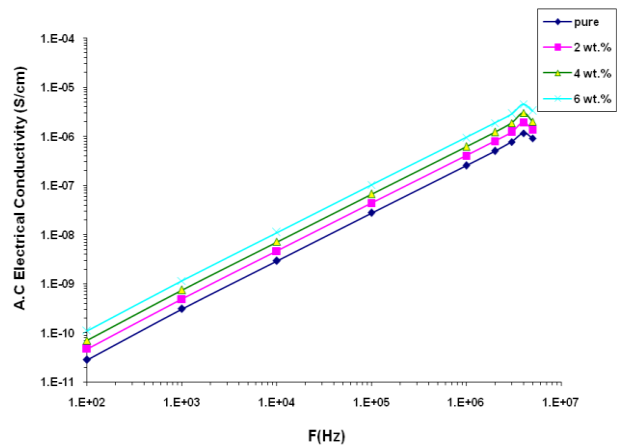


**Fig. 9.** Variation of electrical conductivity of PVA/PVP/SnO<sub>2</sub> nanostructures with frequency.

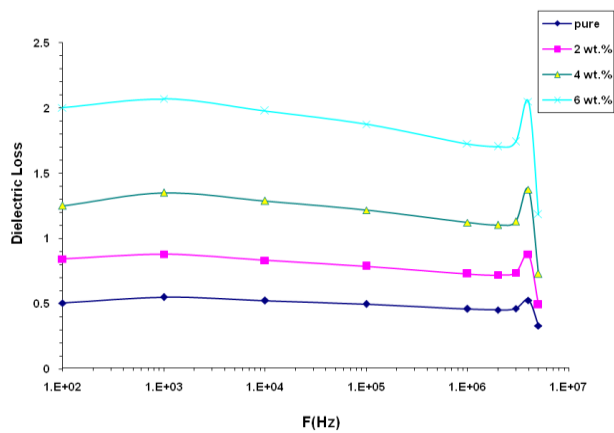


**Fig. 8.** Variation of dielectric losses of PVA/PVP/SnO<sub>2</sub> nanostructures with frequency.

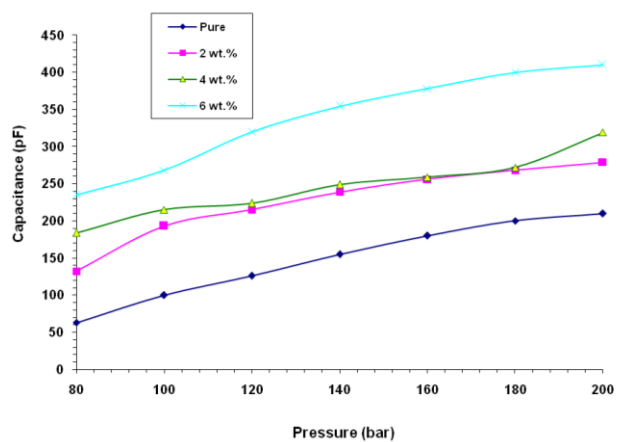


**Fig. 10.** Variation of capacitance for PVA/PVP/SnO<sub>2</sub> nanostructures with pressure.

Figs 7 to 9 show variation of dielectric constant, dielectric losses and electrical conductivity of PVA/PVP/SnO<sub>2</sub> nanostructures with frequency. As shown in figures, the dielectric constant and dielectric losses decrease, and AC electrical conductivity rises with the rise in frequency, this is related to the space charge polarization. The dielectric constant and dielectric losses reduce, and the conductivity rises with the rise in SnO<sub>2</sub> NPs content, this result can be related to the rise in conductivity as a consequence of the rise charge carrier density in the matrix [28] as shown in Fig. 5 where adduced is the distribution of SnO<sub>2</sub> NPs in PVA/PVP blend. The dielectric losses increase at  $f = 4$  MHz. This is due to the highest absorption of applied field. This absorption happens as manifestation of Maxwell–Wagner phenomenon, which is caused by AC current due to the difference of dielectric constant and conductivity of the phases in the composite. This electric current has the same phase as that of the applied field [29, 30].

Fig. 10 represents capacitance variation of PVA/PVP/SnO<sub>2</sub> nanostructures with pressure. As shown in this figure, the capacitance of films rises with the rising pressure. The films contain a crystalline region that has an internal dipole moment. These dipole moments

are randomly oriented without any mechanical or electrical poling process, and the net dipole moment is zero under these conditions. When stress is applied, it changes the local dipole distributions and induces an electric field. The induced electric field accumulates the charges at both bottom and top sides of the film, as a consequence, the capacitance rises [31].

#### 4. Conclusions

This work includes preparing the PVA/PVP/SnO<sub>2</sub> nanostructures and studying the structural, optical and dielectric properties to use them in pressure sensors applications. The results of studying the optical properties have indicated that the absorbance of PVA/PVP blend rises with the increase in SnO<sub>2</sub> NPs content. The energy gap of PVA/PVP blend has been reduced with the rise in SnO<sub>2</sub> NPs content. The absorption coefficient, refractive index and optical conductivity of PVA/PVP blend are increased with the rise in SnO<sub>2</sub> NPs content. The experimental results concerning the dielectric properties have shown that the dielectric constant, dielectric losses and conductivity of PVA/PVP blend increase with the rise in SnO<sub>2</sub> NPs content. The dielectric constant and dielectric losses are reduced,

while the conductivity rises with frequency. The pressure sensors application results have shown that the PVA/PVP/SnO<sub>2</sub> nanostructures have a good sensitivity to pressure.

## References

1. Meshram V.P., Suryavanshi B.M. Electrical characterization of pure and doped with ferric chloride polyvinyl alcohol. *Int. J. Adv. Sci. Eng. Techn.* 2015. Special Issue 1. P. 171–175.
2. Tyagi C. and Sharma A. Linear and monlinear optical study of pure PVA and CdSe doped PVA nanocomposite. *AIP Conf. Proc.* 2016. **1728**. P. 020151. <https://doi.org/10.1063/1.4946202>.
3. Sivaiah K., Kumar K.N., Naresh V., Buddhudu S. Structural and optical properties of Li<sup>+</sup>:PVP & Ag<sup>+</sup>:PVP polymer films. *Materials Sciences and Applications*. 2011. **2**, No 11. P. 1688–1696. <https://doi.org/10.4236/msa.2011.211225>.
4. Saleh S.A., Ibrahim A.A. and Mohamed S.H. Structural and optical properties of nanostructured Fe-doped SnO<sub>2</sub>. *Acta Physica Polonica A*. 2016. **129**, No 6. P. 1220–1225. <https://doi.org/10.12693/APhysPolA.129.1220>.
5. Keskenler E.F., Turgut G., Aydin S., Dilber R., Turgut U. Investigation of boron and yttrium doping effect on structural, electrical and optical properties of sol-gel spin coated SnO<sub>2</sub>. *Journal of Ovonic Research*. 2013. **9**, No 2. P. 61–71.
6. Ikhmayies S.J. Properties of SnO<sub>2</sub>:F thin films prepared by using HF or NH<sub>4</sub>F after exposure to atmosphere. *J. Energy Systems*. 2017. **1**, No 3. P. 120–128. <https://doi.org/10.30521/jes.360535>.
7. Panda S., Acharya B. PDMS/MWCNT nanocomposites as capacitive pressure sensor and electromagnetic interference shielding materials. *J. Mater. Sci.: Mater. Electron.* 2021. **32**. P. 16215–16229. <https://doi.org/10.1007/s10854-021-06170-4>.
8. Khanduri P., Joshi A., Panwar L.S., Goyal A., Panwar V. Sensing performance of ionic polymer metal nanocomposite sensors with pressure and metal electrolytes for energy harvesting applications. In: Hura G., Singh A., Siong L. (eds). *Advances in Communication and Computational Technology*. Lecture Notes in Electrical Engineering. 2021. **668**. Springer. [https://doi.org/10.1007/978-981-15-5341-7\\_63](https://doi.org/10.1007/978-981-15-5341-7_63).
9. Huang P., Xu S., Fu H. *et al.* Fluorescent pressure sensor based on TiO<sub>2</sub>/carbon quantum dots bifunctional nanocomposite film. *J. Mater. Sci.: Mater. Electron.* 2021. **32**. P. 6487–6497. <https://doi.org/10.1007/s10854-021-05366-y>.
10. Al-Attayah K.H.H., Hashim A., Obaid S.F. Fabrication of novel (carboxy methyl cellulose–polyvinylpyrrolidone–polyvinyl alcohol)/lead oxide nanoparticles: structural and optical properties for gamma rays shielding applications. *Int. J. Plastics Technol.* 2019. **23**, No 1. P. 39–41. <https://doi.org/10.1007/s12588-019-09228-5>.
11. El-Sayd E.A., Ibrahiem A.A., Ahmed R.M. Effect of cobalt chloride on the optical properties of PVA/PEG blend. *Arab J. Nucl. Sci. Appl.* 2019. **52**. P. 22–32. <https://doi.org/10.21608/AJNSA.2018.2768.1049>
12. Hashim A., Al-Khafaji Y., Hadi A. Synthesis and characterization of flexible resistive humidity sensors based on PVA/PEO/CuO nanocomposites. *Trans. Electr. Electron. Mater.* 2019. **20**. P. 530–536. <https://doi.org/10.1007/s42341-019-00145-3>.
13. El-Sayed N.M. and Farag O.F. Optical and electrical properties of plasma surface treated polymethylmethacrylate films. *Arab J. Nucl. Sci. Appl.* 2019. **52**, No 4. P. 83–92. <https://doi.org/10.21608/AJNSA.2019.7116.1168>.
14. Hashim A., Al-Attayah K.H.H., Obaid S.F. Fabrication of novel (biopolymer blend-lead oxide nanoparticles) nanocomposites: Structural and optical properties for low cost nuclear radiation shielding. *Ukr. J. Phys.* 2019. **64**, No 2. P. 157–163. <https://doi.org/10.15407/ujpe64.2.157>.
15. Job C.B. Growth, structural, optical, thermal and photo conductivity studies of potassium hepta fluoro antimonate crystals. *Archives of Applied Science Research*. 2015. **7**, No 5. P. 118–128.
16. Jebur Q.M., Hashim A., Habeeb M.A. Structural, electrical and optical properties for (polyvinyl alcohol–polyethylene oxide–magnesium oxide) nanocomposites for optoelectronics applications. *Trans. Electr. Electron. Mater.* 2019. **20**. P. 334–343. <https://doi.org/10.1007/s42341-019-00121-x>.
17. Hashim A., Hamad Z.S. Lower cost and higher UV-absorption of polyvinyl alcohol/silica nanocomposites for potential applications. *Egypt. J. Chem.* 2020. **63**, No 2. P. 461–470. <https://doi.org/10.21608/EJCHEM.2019.7264.1593>.
18. Salohub A.O., Voznyi A.A., Klymov O.V. *et al.* Determination of fundamental optical constants of Zn<sub>2</sub>SnO<sub>4</sub> films. *SPQEO*. 2017. **20**, No 1. P. 79–84. <https://doi.org/10.15407/spqeo20.01.079>.
19. Hadi A., Hashim A., Al-Khafaji Y. Structural, optical and electrical properties of PVA/PEO/SnO<sub>2</sub> new nanocomposites for flexible devices. *Trans. Electr. Electron. Mater.* 2020. **21**, No 3. P. 283–292. <https://doi.org/10.1007/s42341-020-00189-w>.
20. Hashim A., Hadi A. A novel piezoelectric materials prepared from (carboxymethyl cellulose-starch) blend-metal oxide nanocomposites. *Sensor Lett.* 2017. **15**, No 12. P. 1019–1022. <https://doi.org/10.1166/sl.2017.3910>.
21. Shubha L.N., and Madhusudana Rao P. Temperature characterization of dielectric permittivity and AC conductivity of nano copper oxide-doped polyaniline composite. *J. Adv. Dielectr.* 2016. **6**. P. 1650018. <https://doi.org/10.1142/S2010135X16500181>.
22. Hashim A., Habeeb M.A., and Hadi A. Synthesis of novel polyvinyl alcohol–starch-copper oxide nanocomposites for humidity sensors applications with different temperatures. *Sensor Lett.* 2017. **15**, No 9. P. 758–761. <https://doi.org/10.1166/sl.2017.3876>.

23. Hashim A. and Hamad Z.S. Fabrication and characterization of polymer blend doped with metal carbide nanoparticles for humidity sensors. *J. Nanostruct.* 2019. **9**, No 2. P. 340–348. <https://doi.org/10.22052/JNS.2019.02.016>.
24. El-Desoky M.M., Morad I.M., Wasfy M.H., Mansour A.F. Structural and optical properties of TiO<sub>2</sub>/PVA nanocomposites. *IOSR J. Appl. Phys.* 2017. **9**, Issue 5. Ver. III. P. 33–43. <https://doi.org/10.9790/4861-0905033343>.
25. Hashim A., Habeeb M.A., Khalaf A., and Hadi A. Fabrication of (PVA-PAA) blend-extracts of plants bio-composites and studying their structural, electrical and optical properties for humidity sensors applications. *Sensor Lett.* 2017. **15**. P. 589–596. <https://doi.org/10.1166/sl.2017.3856>.
26. Hashim A. Enhanced structural, optical, and electronic properties of In<sub>2</sub>O<sub>3</sub> and Cr<sub>2</sub>O<sub>3</sub> nanoparticles doped polymer blend for flexible electronics and potential applications. *Journal of Inorganic and Organometallic Polymers and Materials.* 2020. **30**, No 2. P. 3894–3906. <https://doi.org/10.1007/s10904-020-01528-3>.
27. Miqdad H. Effect of carbon black nanoparticles on the optical properties of poly (ethylene oxide) films. *Int. J. Appl. Eng. Res.* 2018. **13**, No 6. P. 4333–4341.
28. Ahmed H., Hashim A. Fabrication of PVA/NiO/SiC nanocomposites and studying their dielectric properties for antibacterial applications. *Egypt. J. Chem.* 2020. **63**, No 3. P. 805–811. <https://doi.org/10.21608/EJCHEM.2019.11109.1712>.
29. Bishai A.M., AL-Khayat B.H.F., Awni F.A. Dielectric and physicomechanical properties of electrical porcelain bodies. *Am. Ceram. Soc. Bull.* 1985. **64**, No 4. P. 598–601.
30. Basavaraja C., Choi Y.M., Park H.T. *et al.* Preparation, characterization and low frequency a.c. conduction of polypyrrole-lead titanate composites. *Bull. Korean Chem. Soc.* 2007. **28**, No 7. P. 1104–1108.
31. Hassan D., Hashim A. Synthesis of (poly-methyl methacrylate-lead oxide) nanocomposites and studying their AC electrical properties for piezoelectric applications. *Bull. Electr. Eng. Inform.* 2018. **7**, No 4. P. 547–551. <https://doi.org/10.11591/eei.v7i4.969>.

#### Authors and CV



**Alaa J. Kadham Algidsawi**, Assistant Professor in Solid State and Materials Physics, Assistant Professor at Department of Soil and Water Resources, College of Agriculture, Al-Qasim Green University. The area of her scientific interests includes composites material, polymer composites, nanotechnology.

She has published many scientific researches in international journals indexed in approved global databases. E-mail: a.1978@agre.uoqasim.edu.iq.



**Ahmed Hashim**, Professor, PhD in Materials Physics, Professor at the Department of Physics, University of Babylon, Iraq. The area of his scientific interests includes nanocomposites, semiconductors, sensors, electronics, biomaterials, nanomaterials, composites, nanofluid, polymers, optoelectronics

applications. He has more than 300 papers and 12 patents. H-index = 31 (Scopus), and H-index = 32 (Google scholar).



**Aseel Hadi**, Assistant Professor, PhD in materials engineering, Assistant Professor at the Department of Ceramic and Building Materials, College of Materials Engineering, University of Babylon, Iraq. The area of her scientific interests includes nanomaterials, nanocomposites, nano-

ceramics, sensors, electronics, nanofluid, polymers, optoelectronics applications. She has more than 25 papers. E-mail: aseel16484@yahoo.com.



**Majeed Ali Habeeb**, Professor, PhD in Solid State Physics, Professor at the Department of Physics, College of Education for Pure Sciences, University of Babylon, Iraq. The area of his scientific interests includes nanocomposites, semiconductors, nanomaterials, composites, polymers.

He has more than 70 papers and 4 patents.

#### Дослідження характеристик органічної суміші, легованої наночастинками SnO<sub>2</sub>, для недорогих застосувань у нанoeлектроніці

**A.J.K. Algidsawi, A. Hashim, A. Hadi, M.A. Habeeb**

**Анотація.** Плівкові наноструктури PVA/PVP/SnO<sub>2</sub> виготовляли методом лиття. Досліджено структуру, діелектричні та оптичні характеристики наноструктур PVA/PVP/SnO<sub>2</sub> для датчиків тиску. Результати дослідження діелектричних характеристик показали, що діелектрична проникність, діелектричні втрати та електропровідність суміші підвищуються зі збільшенням вмісту наночастинок SnO<sub>2</sub>. Діелектрична проникність і діелектричні втрати зменшуються, у той час як провідність зростає зі збільшенням частоти. Діелектрична проникність збільшується з 2,53 до 7,41, а діелектричні втрати зростають з 0,5 до 2, тоді як провідність зростає з 2,82·10<sup>-11</sup> до 1,11·10<sup>-10</sup> С/см. Результати дослідження оптичних характеристик показали, що поглинання зростає зі збільшенням вмісту наночастинок SnO<sub>2</sub>. Ширина забороненої зони суміші зменшується з 4,9 до 4,65 eV зі збільшенням вмісту наночастинок SnO<sub>2</sub>. Оптичні константи покращуються зі збільшенням вмісту наночастинок SnO<sub>2</sub>. Результати досліджень датчика тиску показали, що ємність зростає зі збільшенням тиску.

**Ключові слова:** SnO<sub>2</sub>, датчики тиску, ємність, енергетична зона, нанокомпозити.